J. Fluid Mech. (1985), *vol.* 158, *pp.* 95–111
Printed in Great Britain

Marginal separation of a three-dimensional boundary layer on a line of symmetry

By S. N. BROWN

Department of Mathematics, University College London, Gower Street, London WC1E 6BT

(Received 20 August 1984)

The marginal separation of a laminar incompressible boundary layer on the line of symmetry of a three-dimensional body is discussed. The interaction itself is taken to be quasi-two-dimensional but the results differ from those for a two-dimensional boundary layer in that the effect of the gradient of the crossflow is included. Solutions of the resulting integral equation are computed for two values of the additional parameter, and comparisons made with an analytical prediction of the asymptotic form as the length of the separation bubble tends to infinity. The occurrence of the phenomenon is confirmed by an examination of the results of an existing numerical integration of the boundary-layer equations for the line of symmetry of a paraboloid.

1. Introduction

In what is now regarded as a classic paper, Stewartson (1970) showed that it was impossible to remove the Goldstein (1948) singularity at separation in a two-dimensional laminar boundary layer in an adverse pressure gradient by means of a triple deck. This means that in general the notion of an attached flow in which viscous effects are confined to a thin layer in the neighbourhood of the body is inappropriate, and in particular that, when the flow is subsonic and the body is bluff, the external inviscid flow is given by Kirchhoff free-streamline theory (Sychev 1972; Smith 1977). For a supersonic flow the analogous configuration is the self-induced separation discussed by Stewartson & Williams (1969). If, however, the separation is marginal, in the sense that the skin friction just vanishes but immediately recovers, Stewartson, Smith & Kaups (1982) have shown that an interaction region centred on the separation point x_s^* is possible and that the discontinuity in gradient of the skin friction at this point is smoothed out in a region of lateral extent $O(lR^{-\frac{1}{8}})$. The authors had in mind the flow of a uniform stream of speed U_∞ past a blunt-nosed two-dimensional airfoil of chord length l at a critical angle of incidence, where $R = U_\infty l/\nu$ is the Reynolds number and is assumed to be large. They showed that in the interaction region, of triple-deck form, the non-dimensional skin friction satisfies a nonlinear integral equation involving an arbitrary parameter Γ, which the authors interpreted as being proportional to the excess of the angle of incidence over the critical angle. Certain positive values of Γ admit solutions with a region of reversed flow that is of finite length in the variable $R^{\frac{1}{8}}x^*/l$, where x^* measures distance along the airfoil, and the authors showed that for given $0 < \Gamma < 2.76$ the solution is not unique. For $\Gamma > 2.76$ there is no solution, a fact that prevents a possible continuous transition from the attached flow under consideration to a Kirchhoff free-streamline flow. Had Γ tended to infinity with the length of the separation bubble, the flow upstream and downstream of the interaction region would have been able to support a skin friction that was well below marginal. The integral equation

was further studied by Brown & Stewartson (1983, hereinafter referred to as I), where the results of the earlier authors regarding non-uniqueness were confirmed, and the asymptotic form of the solution obtained as the non-dimensional length X_0 of the separation region tended to infinity. Solutions of the unsteady form of the integral equation have been obtained by Smith (1982), who discussed the relevance of the breakdown that he finds at finite time to the occurrence of dynamic stall.

The present investigation extends the results of I to the marginal separation on the line of symmetry of a three-dimensional body at angle of incidence α_0 in a uniform stream. The phenomenon is evident in the computations of Cebeci, Khattab & Stewartson (1980) for the boundary layer near the nose of a paraboloid. When $\alpha_0 = 40°$ the streamwise skin friction dips linearly to zero at one point and then becomes positive again with a rapid increase from a negative to a positive gradient. However, when $\alpha_0 = 41°$ the separation is catastrophic and terminates the computation (see also Nishikawa & Yasui 1984 for the additional effects of slenderness). Here we examine the neighbourhood of this marginal separation point and study the integral equation appropriate to a two-dimensional interaction, which differs from the equation considered in I in that it contains a parameter c_1 measuring the direction and strength of the gradient of the crossflow. It would have been desirable to have allowed the interaction itself to have been three-dimensional, and indeed it is not difficult to set up the relevant equations. However, as the solution was not carried out for the more general case, the simpler situation is considered *ab initio*. The resulting quasi-two-dimensional configuration has some features in common with the study of Smith (1978) of the separation of a vortex sheet from a non-slender body in which a crossflow is accounted for but the appropriate triple-deck is two-dimensional. In fact there have been few fully three-dimensional triple-deck calculations. Smith, Sykes & Brighton (1977) considered a two-dimensional boundary layer encountering a three-dimensional hump, but subsequently linearized the governing equations, as did Smith & Gajjar (1984) in their discussion of flow past wing–body junctions. The calculations of Vatsa & Werle (1977) for supersonic flows over a swept wing were quasi-three-dimensional. Viscous–inviscid interactions on axisymmetric bodies have recently been studied by Kluwick, Gittler & Bodonyi (1984) for supersonic flow and by Duck (1984) for subsonic flow.

The plan of the present paper is as follows. In §§2 and 3 we present the equations and describe the Goldstein solution upstream and downstream of the separation point. This was felt to be desirable as, unlike the two-dimensional situation, the boundary layer downstream of this point must be considered in two parts with an inner and an outer Goldstein region. The interaction region at x_s^* smoothes out the discontinuity in the non-dimensional streamwise skin friction, which is of the form $\tau_1(x_s^*-x^*)/l$ as $x^*\to x_s^{*-}$ and $\tau_2(x^*-x_s^*)/l$ as $x^*\to x_s^{*+}$, where τ_1 and τ_2 are constants. In §4 the interaction region is discussed, and the relevant integral equation, which reduces to that of I as $\tau_2\to\tau_1$, is obtained. Numerical solutions of the equation are derived in §5 for the values $\lambda = 0.75$ and 1.25, where $\lambda = \tau_2/\tau_1$. These are more difficult to compute than for the case $\lambda = 1$ as the boundary conditions for the integral equation are no longer symmetric in $x^*-x_s^*$. Thus the parameter Γ of I is replaced by two related but unequal parameters $\Gamma_\pm$. A non-uniqueness similar to that of I is again evident, and it is found that, as X_0, the length of the separation bubble, tends to infinity, $\Gamma_+\to\infty$ if $\lambda > 1$ but $\Gamma_+\to-\infty$ if $\lambda < 1$. However, $\Gamma_-\to 0$, as does Γ in I.

Asymptotic solutions supporting the predictions concerning $\Gamma_\pm$ are presented in §6, where in addition it is shown that the solution of the integral equation is

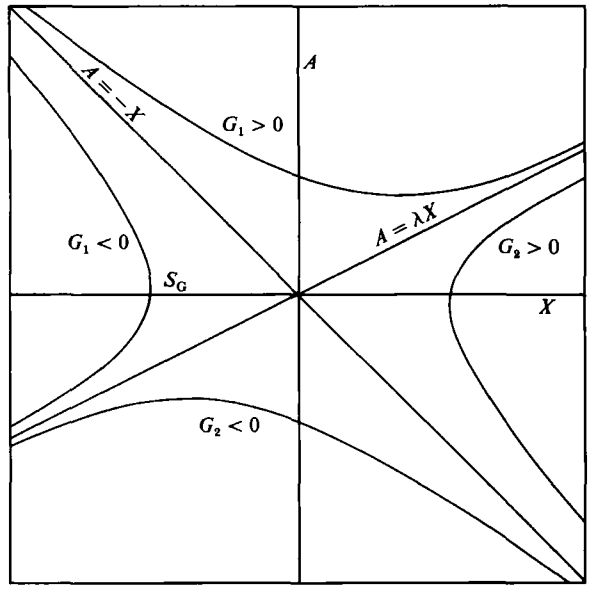

FIGURE 1. Illustration of the solutions of (1.1) for the case $\lambda < 1$. The case $\lambda > 1$ is similar.

approaching the same limit solution discussed in I for the case $\lambda = 1$, as indicated by the numerical work. In §7 we consider the application of the theory to the calculations of Cebeci *et al.* (1980), which, it is shown, correspond to the situation $\lambda < 1$.

Interpretation of the constants $\Gamma_{\pm}$ is less obvious than in the case $\lambda = 1$, when they are equal and may sensibly be related to the angle of incidence. We find that, as the distance X from the separation point, defined by $X = R_\delta^{\frac{1}{3}}(x^* - x_s^*)/l$, becomes large, the effect of the interaction decreases, and the suitably scaled skin friction $A(X)$ satisfies the equation

$$A\frac{\mathrm{d}A}{\mathrm{d}X} = \lambda X - (1-\lambda)A. \tag{1.1}$$

Equation (1.1) has a saddle point at $A = X = 0$, and solutions are sketched in figure 1, where the constants G_1 and G_2 are used for solutions respectively above and below the line $A = \lambda X$. Thus

$$(A+X)(A-\lambda X)^{\lambda} = G_1, \quad (A+X)(\lambda X - A)^{\lambda} = G_2. \tag{1.2a,b}$$

When $G_1 > 0$ solutions proceed from $X = -\infty$, where $A \approx -X$, to $X = +\infty$, where $A \approx \lambda X$, in a regular manner with the flow attached. For these solutions the angle of incidence is below critical. When $G_1 < 0$, A possesses a classical Goldstein square-root singularity at the point S_G, and catastrophic breakdown occurs. The interaction modifies the situation of figure 1 and, more importantly, bridges the gap between solutions with $G_1 < 0$ and those with $G_2 > 0$. It enables the question to be asked 'How negative may G_1 be and how positive may G_2 be for this bridging still to be possible?' A strongly negative G_1 means that the skin friction is significantly below its Goldstein value far upstream, while a strongly positive G_2 means that it is well below the corresponding value far downstream. Indeed

$$A \approx -X + \frac{G_1}{(-X)^{\lambda}(1+\lambda)^{\lambda}} \quad \text{as } X \to -\infty \tag{1.3a}$$

and $$A \approx \lambda X - \left(\frac{G_2}{X(1+\lambda)}\right)^{1/\lambda} \quad \text{as } X \to \infty. \tag{1.3b}$$

We will ignore the solutions on which G_2 is negative, as these correspond to already separated flows; examples are noted in I and are more extensively discussed by Rhyzhov & Smith (1985). When the terms due to the interaction are included in (1.1), A again has the asymptotic forms of (1.3a, b), but instead we write, by analogy with I,

$$A \approx -X - \frac{\Gamma_-}{2(-X)^\lambda} \quad \text{as } X \to -\infty, \tag{1.4a}$$

$$A \approx \lambda X - \frac{\Gamma_+}{2X^{1/\lambda}} \quad \text{as } X \to \infty, \tag{1.4b}$$

so that significantly positive $\Gamma_\pm$ would perhaps give a possibility of a match with a grossly separated Kirchhoff free-streamline solution. The parameters $\Gamma_\pm$, which were equal in I, are here unequal but related. Equation (1.1) represents the limit $\Gamma_\pm \to -\infty$.

At first it might appear that a breakthrough has been made in the search for a continuous transition from an attached inviscid solution to a Kirchhoff free-streamline solution because, when $\lambda > 1$, $\Gamma_+ \to \infty$ as $X_0 \to \infty$, and therefore the flow downstream of the interaction region, with which this solution must match, can support a skin friction that is an order of magnitude lower than that predicted by the leading-order Goldstein solution. However, when $\lambda > 1$ this effect on the downstream flow is, in terms of Reynolds number $O(R^{-\frac{1}{8}(1+1/\lambda)})$ and therefore small. In addition, we have been unable to find examples of a flow along a line of symmetry with $\lambda > 1$, corresponding to an influx of the secondary velocity, except for the favourable-pressure-gradient situations of Stewartson & Simpson (1982) and Cebeci, Stewartson & Brown (1983), to which form of singularity this theory does not apply. Also we have not considered the limits $\lambda \to 0$ and $\lambda \to \infty$, which promise to be of mathematical if not of great physical interest.

2. The geometry and the equations of motion

We consider the flow of an incompressible fluid of kinematic viscosity ν in the neighbourhood of the line of symmetry $y = z = 0$ on a surface $y = 0$, and to avoid undue complication we shall assume that near the point of marginal separation S on the line it is sufficient to consider the body to be plane. Now the solution of the boundary-layer equations along the line of symmetry may be calculated independently of the flow over the rest of the body, since the pressure gradients are prescribed, but this is not true for the solution of the Navier–Stokes equations because of the pressure gradient normal to the line of symmetry. However, if we restrict ourselves to a two-dimensional interaction so that the induced pressure gradient is independent of z, we may confine our investigations to the plane $z = 0$. We let l be a typical length, say the distance of S from an upstream stagnation point on this line, let U_∞ be the uniform speed at infinity of the fluid, and take Cartesian coordinates (lx, ly, lz) with origin at S and corresponding velocity components

$$U_\infty\{u(x,y) + O(z^2),\ v(x,y) + O(z^2),\ zw(x,y) + O(z^3)\}, \tag{2.1a}$$

and pressure $$\rho U_\infty^2\{p(x,y) + \tfrac{1}{2}z^2 s(x) + O(z^4)\}. \tag{2.1b}$$

Here u, v, w and p will, in the interaction region centred on S, differ from their boundary-layer values, but $s(x)$ will not, since the perturbation to the pressure is

assumed to be independent of z. Thus s is determined from the potential flow and is independent of the normal coordinate y. This means that for our purposes it is sufficient to consider the Navier–Stokes equations in the limit $z \to 0$ as

$$\operatorname{div} \boldsymbol{q} + w = 0, \tag{2.2a}$$

$$(\boldsymbol{q}\cdot\boldsymbol{\nabla})\,\boldsymbol{q} = -\boldsymbol{\nabla} p + R^{-1}\boldsymbol{\nabla}^2\boldsymbol{q}, \tag{2.2b}$$

$$\boldsymbol{q}\cdot\boldsymbol{\nabla} w + w^2 = -s + R^{-1}\boldsymbol{\nabla}^2 w, \tag{2.2c}$$

where s is given. Here $\boldsymbol{q} = (u, v)$, all the vector operators are two-dimensional in the plane of symmetry (x, y), and $R = U_\infty l/\nu$ is the Reynolds number, assumed to be large.

In the following we take $R \gg 1$ and, except when x is within a distance $O(R^{-\frac{1}{8}})$ of S, (2.2) reduce to the conventional boundary-layer equations. In this region an interaction takes place between the boundary layer and the outer inviscid flow and the solution is of triple-deck form. However, we first set out the relevant properties of the flow upstream and downstream of S, where the solution in the boundary layer of thickness $O(R^{-\frac{1}{2}})$ in y is controlled by the external inviscid flow $\{u_e(x), 0, w_e(x)\}$. This is required to establish the conditions that are to be satisfied by the solution in the interaction region, which must match with the Goldstein solution upstream and downstream. In I the Goldstein skin friction was symmetric about S, but this is not so in the presence of crossflow.

3. The solution upstream and downstream of the marginal separation point

The flow that approaches S, the point of zero streamwise skin friction, from upstream is a standard viscous boundary layer of thickness $O(R^{-\frac{1}{2}})$. We do, however, make the assumption that, to leading order, the skin friction τ vanishes in a regular fashion at S and that the Goldstein square-root singularity is absent. In fact $\tau \propto |x|$ both as $x \to 0\mp$, and the interaction region centred on S serves to smooth out this discontinuity in slope. If, either upstream or downstream of S, the skin friction contains, at any order, non-integral powers of x as $|x| \to 0$, it is necessary to divide the boundary layer into its outer and inner Goldstein regions. In the outer region the appropriate variables are x and $R^{\frac{1}{2}}y$, and in the inner they are $|x|^{\frac{1}{4}}$ and $R^{\frac{1}{2}}y/|x|^{\frac{1}{4}}$. If the inner region is unnecessary, because the solution in the outer region satisfies the boundary conditions on the wall, we shall term this a regular Goldstein expansion. In the following we shall ask, at least to the order in $|x|$ that has any influence on the interaction region, that the solution upstream of S is regular. However, we shall find that the interaction region forces the solution downstream of it to be singular and require both an inner as well as an outer Goldstein region. This did not occur in the two-dimensional case of I, where the boundary-layer flow was symmetric about S.

In the boundary layer that approaches or leaves S we take $x = O(1)$, $u = O(1)$, $w = O(1)$ and set

$$y = R^{-\frac{1}{2}}Y, \quad v = R^{-\frac{1}{2}}V \tag{3.1}$$

in (2.2) and let $R \to \infty$ to obtain the conventional boundary-layer equations for a line of symmetry:

$$\frac{\partial u}{\partial x} + \frac{\partial V}{\partial Y} + w = 0, \quad u\frac{\partial u}{\partial x} + V\frac{\partial u}{\partial Y} = -\frac{\partial p}{\partial x} + \frac{\partial^2 u}{\partial Y^2}, \tag{3.2a,b}$$

$$0 = -\frac{\partial p}{\partial Y}, \quad u\frac{\partial w}{\partial x} + V\frac{\partial w}{\partial Y} + w^2 = -s + \frac{\partial^2 w}{\partial Y^2}, \tag{3.2c,d}$$

for which the boundary conditions are

$$\left.\begin{aligned} u = V = w = 0 \quad &\text{on } Y = 0, \\ u \to u_e(x), \quad w \to w_e(x) \quad &\text{as } Y \to \infty, \end{aligned}\right\} \tag{3.3a}$$

and also

$$-\frac{\partial p}{\partial x} = u_e(x)\,u_e'(x), \quad -s = u_e(x)\,w_e'(x) + w_e^2(x). \tag{3.3b}$$

For the outer Goldstein solution that approaches or leaves S we allow for the possibility of an inner flow by not requiring that the no-slip condition is satisfied at all orders of the expansion. We expand u, V and w in powers of x with coefficients that are functions of Y as follows:

$$\begin{aligned} u = {} & U_0(Y) - x\{V_1'(Y) + W_1(Y) + \mu U_0'(Y)\} \\ & - \tfrac{1}{2}x^2\{V_2'(Y) + W_2(Y) - 2\mu(V_1''(Y) + W_1'(Y)) - \mu^2 U_0''(Y)\} + o(x^2), \end{aligned} \tag{3.4a}$$

$$V = V_1(Y) + \mu U_0(Y) + x\{V_2(Y) - \mu(2V_1'(Y) + W_1(Y)) - \mu^2 U_0'(Y)\} + o(x), \tag{3.4b}$$

$$w = W_1(Y) + x\{W_2(Y) - \mu W_1'(Y)\} + o(x), \tag{3.4c}$$

$$p = P_0 + P_1 x + \tfrac{1}{2}P_2 x^2 + o(x^2), \quad s = Q_2 + o(1). \tag{3.4d}$$

Here Q_2 and the P_i are given constants, and $U_0(Y)$ and $W_1(Y)$ are the streamwise and crossflow velocity profiles at S and are determined partly by the history of the boundary layer and partly, as we shall see below, by requirements of regularity of the successive terms in (3.4). Also, μ is a constant, to be chosen later, which will have a different value according as $x \lesseqgtr 0$. We write

$$U_0(Y) = \sum_{n=2}^{8} \frac{a_n Y^n}{n!} + o(Y^8), \quad W_1(Y) = \sum_{n=1}^{5} \frac{c_n Y^n}{n!} + o(Y^5) \tag{3.5}$$

with $a_2 > 0$, where in addition it is assumed that $U_0(Y) \to u_e(0)$, $W_1(Y) \to w_e(0)$ as $Y \to \infty$. It may be noted that (3.4*a–c*) satisfy the continuity equation of (3.2).

When V_1 is determined from (3.2*b*) subject to the conditions $V_1(0) = V_1'(0) = 0$, so that (3.4*a*) satisfies the no-slip condition to $O(x)$, the requirement that V_1 is regular at $Y = 0$ leads to the following restrictions on $U_0(Y)$:

$$a_2 = P_1, \quad a_3 = a_4 = 0, \quad a_5 = -3a_2 c_1. \tag{3.6}$$

In addition, the constant of integration in the equation for V_1 is chosen, for convenience, to make $V_1''(0) = -c_1$, so that, for small x, the streamwise skin friction τ is such that $\tau \approx -\mu a_2 x$.

The equation for W_2 is obtained from (3.2*d*), and implies restrictions on the crossflow velocity profile W_1. These are

$$c_2 = Q_2, \quad c_3 = 0, \quad c_4 = c_1^2 + a_2\beta, \tag{3.7}$$

where $\beta = W_2(0)$, which is not necessarily zero. Finally, if V_2 is to be regular with $V_2(0) = 0$ it is necessary that, in addition,

$$a_6 = 2a_2(P_2 - 2Q_2), \quad a_7 = 0 \tag{3.8}$$

and

$$\frac{1}{9}\frac{a_8}{a_2} = \tfrac{13}{3}c_1^2 + a_2(\alpha - \tfrac{5}{3}\beta), \tag{3.9}$$

where $\alpha = V_2'(0)$.

To summarize thus far, we see that, if the assumed forms (3.4) are to be regular for small Y, have zero normal velocity on $Y = 0$ and satisfy the no-slip condition to

$O(1)$ in the crossflow and to $O(x)$ in the streamwise flow, then U_0 and W_1 have only a_2 and c_1 arbitrary up to and including the terms $O(Y^8)$ in U_0 and $O(Y^4)$ in W_1. This is on the assumption that μ, α and β are given, the reason for which is now explained.

Let us suppose that on the upstream side of S the flow is a regular expansion with $u(0) = w(0) = 0$ and does not require, at least to the order in x considered here, an inner Goldstein expansion. This implies that $\beta = \mu c_1$, $\alpha + \beta = \mu^2 a_2$, and, if the skin friction as $x \to 0-$ is $-\tau_1 x$, so that $\mu = \tau_1/a_2$, then (3.7) and (3.9) lead to

$$c_4 = c_1^2 + c_1\tau_1, \quad \frac{1}{9}\frac{a_8}{a_2} = \tau_1^2 - \tfrac{8}{3}c_1\tau_1 + \tfrac{13}{3}c_1^2, \tag{3.10}$$

and c_4 and a_8 are determined in terms of the oncoming-flow properties a_2, c_1 and τ_1. Downstream of the interaction region we assume that the flow is also described by expansions of the form (3.4), but with a different value of μ. The analysis up to (3.9) is still valid, and so are the relations (3.10) on the coefficients of the separation profiles. We note that (3.7), (3.9) and (3.10) lead to

$$V_2'(0) = \alpha = \frac{\tau_1}{a_2}(\tau_1 - c_1), \quad W_2(0) = \beta = \frac{c_1\tau_1}{a_2}. \tag{3.11}$$

If we now take $\mu = -\tau_2/a_2$ ($\tau_2 > 0$), so that the flow to the right of the marginal separation region has a skin friction that is linearly increasing downstream, we see from (3.4a, b) that $u(0) = w(0) = 0$ only if $\tau_1^2 = \tau_2^2$ and $c_1(\tau_1 + \tau_2) = 0$. This means that the solution downstream of the separation region can have a regular Goldstein expansion only if $c_1 = 0$ with $\tau_1 = \tau_2$, which is the zero-crossflow case discussed in I. However, if $c_1 \neq 0$, as we are assuming here, an inner Goldstein expansion is required in which the no-slip conditions are satisfied and which, as we shall find, determines the value of τ_2. We note that we are disregarding the case $\tau_2 = -\tau_1$, in which situation a regular Goldstein separation without reattachment occurs.

In the inner layer we write, for $x > 0$,

$$\xi = x^{\frac{1}{4}}, \quad \eta = \frac{Y}{2^{\frac{1}{2}}\xi}, \quad u = \frac{\partial\psi}{\partial Y}, \quad w = \frac{\partial\phi}{\partial Y}, \quad v + \phi = -\frac{\partial\psi}{\partial x} \tag{3.12}$$

in (3.2), followed by

$$\psi = 2^{\frac{3}{2}}\xi^3 f(\xi, \eta), \quad \phi = 2^{-\frac{1}{2}} g(\xi, \eta), \tag{3.13}$$

and expand f and g in powers of ξ with coefficients that are functions of η. It is straightforward to calculate these functions as far as f_5 and g_4, as they are polynomials in η that may be obtained by writing the expansions of the terms of (3.4) with $\mu = -\tau_2/a_2$ for small Y in terms of η. However, the equation for g_5 has a complementary function which leads to a solution (with $g_5'(0) = 0$ to make $w = 0$ on the wall) that includes a contribution $O(\eta)$ for $\eta \gg 1$ that matches with the term $O(x)$ in (3.4a). It may then be verified that the corresponding solution for f_6 with $f_6(0) = f_6'(0) = 0$ gives a match with the appropriate terms in (3.4) provided that

$$\tau_2 = \tau_1 - c_1. \tag{3.14}$$

This relation, which, since $\tau_2 > 0$, implies that $\tau_1 > c_1$, between the gradients of the skin friction as $x \to 0-$ and $x \to 0+$, together with the confirmation that the no-slip condition is satisfied, is the final property of the Goldstein solution required for the discussion to follow of the interaction region.

4. The interaction region

As in I, the appropriate streamwise scale for the interaction region centred on $x = 0$ is $x = O(R^{-\frac{3}{8}})$. In the normal direction the flow is divided into three decks; in the main deck $Y = O(1)$, as in the boundary layers immediately upstream and downstream, in the upper deck $Y = O(R^{\frac{3}{10}})$, so that x and y are of the same order of magnitude, and in the lower deck $Y = O(R^{-\frac{1}{26}})$ with the result that $Y/|x|^{\frac{1}{4}}$ is of order unity, as required for a match with an inner Goldstein region.

To discuss the interaction region we set $\delta = R^{-\frac{1}{8}}$ and

$$x = \delta X, \tag{4.1}$$

in (2.2), so that in the main deck the appropriate variables are X and Y, and the required expressions are easily found to be of the form

$$\begin{aligned} u = {} & U_0(Y) - \delta X(V_1'(Y) + W_1(Y)) - \tfrac{1}{2}\delta^2 X^2(V_2'(Y) + W_2(Y)) \\ & + \delta A(X)\, U_0'(Y) + \delta[\tfrac{1}{2}(A^2+\gamma)\, U_0''(Y) - XA(X)\,(V_1''(Y) + W_1'(Y))] + o(\delta^2), \end{aligned} \tag{4.2a}$$

$$\begin{aligned} V = {} & V_1(Y) + \delta X V_2(Y) - A'(X)\, U_0(Y) \\ & + \delta[XA'(X)\, W_1(Y) + (XA)'\, V_1'(Y) - A(X)\, A'(X)\, U_0'(Y)] + o(\delta), \end{aligned} \tag{4.2b}$$

$$w = W_1(Y) + \delta X W_2(Y) + \delta A(X)\, W_1'(Y) + o(\delta), \tag{4.2c}$$

$$p = P_0 + \delta P_1 X + \tfrac{1}{2}\delta^2 P_2 X^2 + \delta^{\frac{1}{2}}\tilde{P}(X) + o(\delta^{\frac{1}{2}}). \tag{4.2d}$$

The expressions (4.2) are analogous to those in the main deck of I, but require some explanation. The first three terms of (4.2a, d) and the first two of (4.2b, c) are the terms of (3.4) with $\mu = 0$, as these are common to the flow upstream and downstream of the interaction region so are written explicitly in (4.2) for convenience. The functions $A(X)$ and $\tilde{P}(X)$ arise from the interaction and are to be found and must be such that (4.2) matches with (3.4) as $|X| \to \infty$. This means for example that

$$\left.\begin{aligned} A(X) &\approx -\frac{\tau_1 X}{a_2} \quad \text{as } X \to -\infty, \\ A(X) &\approx \frac{\tau_2 X}{a_2} \quad \text{as } X \to \infty. \end{aligned}\right\} \tag{4.3}$$

The constant γ in (4.2a) is arbitrary, and in I was interpreted as a measure of the amount of increase over the critical angle of incidence for marginal separation that was possible. It is not clear that it plays precisely that role here, as this seems to be taken over by another constant of integration, which is identical with γ only in the two-dimensional case. This point, which is considered to be fairly minor, is mentioned again at the end of the section.

Since (4.2a, c) do not satisfy the no-slip conditions on $Y = 0$ an inner deck is necessary, and as in I it is convenient to write the solution there as that in the main deck plus a correction $O(\delta^2)$ in u, and $O(\delta)$ in v and w. Thus, if the correction to u in (4.2) is $\delta^2\tilde{U}(X, \tilde{Y})$ and to v and w, $\delta\tilde{V}(X, \tilde{Y})$ and $\delta\tilde{W}(X, \tilde{Y})$ respectively, where

$$Y = \delta^{\frac{1}{4}}\tilde{Y}, \tag{4.4}$$

then it may be shown, from (2.2), that

$$\frac{\partial \tilde{U}}{\partial X}+\frac{\partial \tilde{V}}{\partial \tilde{Y}}+\tilde{W}=0, \tag{4.5a}$$

$$\tfrac{1}{2}a_2\,\tilde{Y}^2\frac{\partial \tilde{W}}{\partial X}=\frac{\partial^2 \tilde{W}}{\partial \tilde{Y}^2}, \tag{4.5b}$$

$$\tfrac{1}{2}a_2\,\tilde{Y}^2\frac{\partial \tilde{U}}{\partial X}+a_2\,\tilde{Y}\tilde{V}=-\tilde{P}'(X)+\frac{\partial^2 \tilde{U}}{\partial \tilde{Y}^2}, \tag{4.5c}$$

with boundary conditions

$$\tilde{U}(X,\infty)=\tilde{W}(X,\infty)=0, \tag{4.6a}$$

and

$$\left.\begin{aligned}&\tilde{U}(X,0)=\frac{\tau_1^2X^2}{2a_2}-\tfrac{1}{2}(A^2+\gamma)\,a_2,\\ &\tilde{V}(X,0)=0,\quad \tilde{W}(X,0)=-\frac{c_1\tau_1}{a_2}X-c_1A,\end{aligned}\right\} \tag{4.6b}$$

in order that (4.2) plus its correction may satisfy the no-slip conditions. As $X\to-\infty$ it is sufficient at present to assume that

$$\frac{\partial \tilde{U}}{\partial X}+\tilde{W}\to 0. \tag{4.7}$$

The Fourier transform of (4.5*b*) is Weber's equation, and there is a unique exponentially decaying solution that satisfies the boundary conditions. Differentiation of (4.5*c*) with respect to X, addition of (4.5*b*) and subsequent differentiation with respect to $\tilde{Y}$ leads to Stewartson's (1970) problem for $\tilde{V}$ (see the Appendix to that paper), of which an acceptable solution exists only if a certain relation holds between $\tilde{P}$ and A. It is, in this case, that, with $\tau_2=\tau_1-c_1$,

$$\int_{-\infty}^{X}\left(\frac{\tau_1\tau_2}{a_2}X_1-c_1A-a_2AA'\right)\mathrm{d}X_1=\frac{(-\frac{1}{4})!}{a_2^{\frac{1}{2}}2^{\frac{3}{2}}(\frac{1}{4})!}\int_{-\infty}^{X}\frac{\tilde{P}'(X_1)\,\mathrm{d}X_1}{(X_1-X)^{\frac{1}{2}}}. \tag{4.8}$$

The existence of the integral on the left will be verified when the equation for A is found below.

The upper deck leads to a second condition between A and $\tilde{P}$. The solution there is standard and gives, with $U_e=u_e(0)$,

$$\tilde{P}'(X)=\frac{U_e^2}{\pi}\int_{-\infty}^{\infty}\frac{A''(X_1)\,\mathrm{d}X_1}{X-X_1}. \tag{4.9}$$

Elimination of $\tilde{P}$ as in Stewartson (1970) leads to the following equation for A:

$$\int_{-\infty}^{X}\left[a_2AA'+c_1A-\frac{\tau_1\tau_2}{a_2}X_1\right]\mathrm{d}X_1=\frac{U_e^2(-\frac{1}{4})!}{2^{\frac{3}{2}}a_2^{\frac{1}{2}}(\frac{1}{4})!}\int_{X}^{\infty}\frac{A''(X_1)\,\mathrm{d}X_1}{(X_1-X)^{\frac{1}{2}}}. \tag{4.10}$$

The parameters in (4.10) may be reduced to one by linear scaling, and it may then be written as

$$\int_{-\infty}^{X}[AA'-\lambda X_1+(1-\lambda)A]\,\mathrm{d}X_1=\frac{1}{2}\int_{X}^{\infty}\frac{A''(X_1)\,\mathrm{d}X_1}{(X_1-X)^{\frac{1}{2}}}, \tag{4.11}$$

where

$$\lambda=1-\frac{c_1}{\tau_1}\left(\equiv\frac{\tau_2}{\tau_1}\right)>0. \tag{4.12}$$

The conditions that A must satisfy as $|X| \to \infty$ are that

$$\left.\begin{aligned} A(X) &\approx -X \quad \text{as } X \to -\infty, \\ A(X) &\approx \lambda X \quad \text{as } X \to \infty. \end{aligned}\right\} \tag{4.13}$$

The corrections to (4.13) may be found by noting that the integrand on the left-hand side of (4.11) must tend to zero both as $X \to \pm\infty$. This implies that as $|X| \to \infty$

$$(A+X)(A-\lambda X)^{\lambda} \approx G, \tag{4.14}$$

where the constant G is different for positive and negative X. Thus (4.13) may be augmented as in (1.4). The contribution to (1.4) forced by the right-hand side of (4.11) is $O(|X|^{-\frac{3}{2}})$, and is thus more important than the term in Γ_- in (1.4a) if $\lambda > \frac{3}{2}$, and more important than the term in Γ_+ in (1.4b) if $\lambda < \frac{2}{3}$. In the situation of I, which corresponds to $\lambda = 1$, the constants $\Gamma_\pm$ were equal and denoted by Γ. Equation (4.11) may be rewritten in either of the following forms:

$$A^2 - X^2 + \frac{\Gamma_-}{(1+X^2)^{\frac{1}{2}(\lambda-1)}} + 2(1-\lambda)\int_{-\infty}^{X} \left(A + X_1 - \frac{\frac{1}{2}\Gamma_- X_1}{(1+X_1^2)^{\frac{1}{2}(\lambda-1)}}\right) \mathrm{d}X_1 = \int_X^{\infty} \frac{A''(X_1)\,\mathrm{d}X_1}{(X_1 - X)^{\frac{1}{2}}} \tag{4.15a}$$

or, equivalently,

$$A^2 - \lambda^2 X^2 + \frac{\lambda\Gamma_+}{(1+X^2)^{\frac{1}{2}(1/\lambda-1)}} - 2(1-\lambda)\int_X^{\infty} \left(A - \lambda X_1 + \frac{\frac{1}{2}\Gamma_+ X_1}{(1+X_1^2)^{\frac{1}{2}(1/\lambda+1)}}\right) \mathrm{d}X_1 = \int_X^{\infty} \frac{A''(X_1)\,\mathrm{d}X_1}{(X_1 - X)^{\frac{1}{2}}}. \tag{4.15b}$$

The asymptotic forms of A do not permit a constant of integration to be added to either left-hand side except in the case $\lambda = 1$ of I, to which (4.15a, b) both reduce as $\lambda \to 1$. The constants $\Gamma_\pm$ are related, since the left-hand sides of (4.15a, b) must be equal for all values of X; in particular with $X = 0$,

$$\Gamma_- + 2(1-\lambda)\int_{-\infty}^{0} \left(A + X_1 - \frac{\frac{1}{2}\Gamma_- X_1}{(1+X_1^2)^{\frac{1}{2}(\lambda+1)}}\right) \mathrm{d}X_1 = \lambda\Gamma_+ - 2(1-\lambda)\int_0^{\infty} \left(A - \lambda X_1 + \frac{\frac{1}{2}\Gamma_+ X_1}{(1+X_1^2)^{\frac{1}{2}(1/\lambda+1)}}\right) \mathrm{d}X_1. \tag{4.16}$$

5. The numerical solution of the integral equation

Some feeling for the solution of the integral equation is given by its solution when both $\Gamma_\pm$ are large and negative. This is given by neglecting the right-hand side of (4.15), which leads to (1.1), the solution of which is (1.2a) with $G_1 > 0$. From this we obtain

$$-\tfrac{1}{2}\Gamma_+ = (-\tfrac{1}{2}\Gamma_-)^{1/\lambda}(1+\lambda)^{1-1/\lambda}, \tag{5.1}$$

with the result that Γ_+ and Γ_- are equal as required when $\lambda = 1$. In this solution A is always positive and tends to its linear asymptotes from above as $|X| \to \infty$, and if $\lambda = O(1)$ the profile is reasonably symmetric about $X = 0$. To obtain a separated profile in which the skin friction is negative for a finite range of X, either Γ_+ or Γ_- or both must increase and become positive. In these circumstances a numerical solution of (4.15) is required, and this has been carried out for $\lambda = 0.75$, 1.25 by the method described in I. The integral equation was reduced to a set of nonlinear algebraic equations, after A'' was replaced by central differences and the integrals

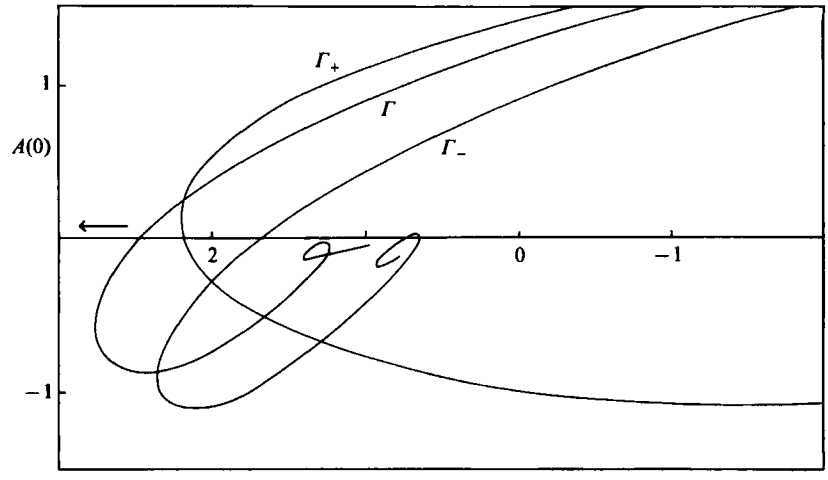

FIGURE 2. The $(\Gamma, A(0))$-plane when $\lambda = 0.75$.

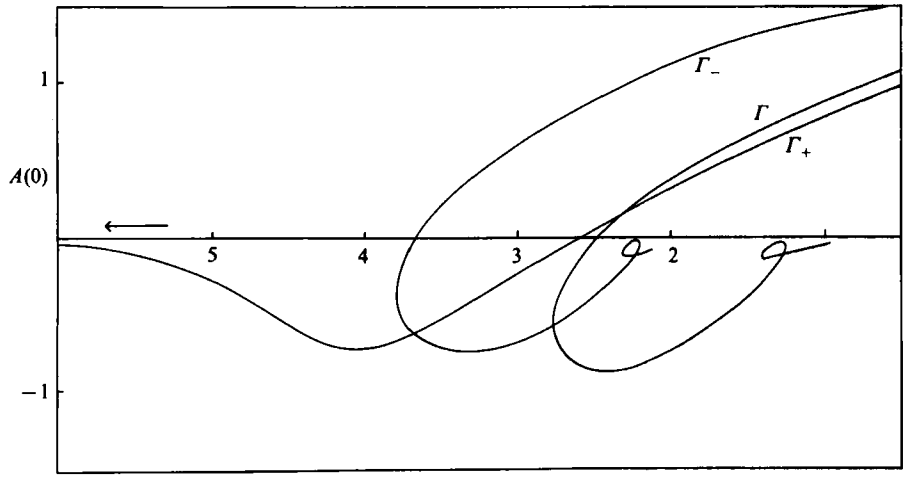

FIGURE 3. The $(\Gamma, A(0))$-plane when $\lambda = 1.25$.

evaluated by an approximate method. For simplicity both integrals were treated the same way: the substitution $X_1 = X + t^2$ was made as in I and then the trapezium rule used. There is a choice between integrating (4.15*a*) and (4.15*b*), the advantage of (4.15*b*) being that the resulting matrix is almost triangular with at most two subdiagonals, so, apart from a few runs to check accuracy, (4.15*b*) was used throughout.

In figures 2 and 3 we show the results of plotting $\Gamma_\pm$ against $A(0)$ for the two values of λ considered. In both figures is also shown, for comparison, the corresponding curve obtained in I with $\lambda = 1$; in that case $\Gamma_+ = \Gamma_-$. It will be noticed that in both cases the curve for Γ_- is similar in shape to that with $\lambda = 1$, and after making a small but definite loop is probably tending to the origin. In the case $\lambda = 1$ it was possible to find the analytic form of Γ in terms of the length of the separation region as Γ tended to zero and the latter tended to infinity. Here, as explained in §6, it has not been found possible to find the analogous formula, though a seemingly consistent expression for Γ_+ has been obtained on the assumption that Γ_- tends to zero. The

main difference between these results and those of I is the behaviour of Γ_+, which when $\lambda = 0.75$ is tending to minus infinity and when $\lambda = 1.25$ tends to plus infinity. Both these asymptotic behaviours are confirmed by the analysis of §6; on both curves $A(0) \to 0$.

The curves of figures 2 and 3 were obtained and traversed as follows. Whichever equation of (4.15) is used with boundary conditions (1.4) essentially one of $\Gamma_\pm$ must be given and the other calculated in terms of it, either by examining the asymptotic form or by using (4.16). Here for example on those parts of the curve where $A(0) > 0$ it was found convenient to use (4.15*b*) with Γ_+ prescribed and to calculate Γ_- from (4.16). In fact the method used was, for given Γ_+, to estimate Γ_-, solve the matrix equations for the values of A at the mesh points by Newton iteration subject to (1.4), recalculate Γ_- from (4.16), re-solve the matrix equations and repeat the cycle until the difference between the results of consecutive cycles was less than a prescribed tolerance. Although, when $\lambda = 1.25$, Γ_+ decreases monotonically, so it would have been possible to compute both curves by prescribing Γ_+, it was found more convenient, as in I, to traverse the curves by increasing X_0, the position of the reattachment point, as soon as X_0 sensibly existed. As X_0 increased, and the region of reversed flow lengthened, the profiles for both values of λ became increasingly non-symmetric, and as in the case $\lambda = 1$ the limit solution for $X < X_0$ seemed to be $A(X) \approx -X$ for $X < X_0$, with a rapid increase from $-X_0$ to X_0 in the neighbourhood of this point.

Some indication of the values of X_0 at various points of the curves of figures 2 and 3 is required. When $\lambda = 0.75$, Γ_+ reaches a maximum of approximately 2.21 where $A(0) \approx 0.07$ and $X_0 \approx 0.93$. The maximum value of Γ_-, approximately 2.33, does not occur until $X_0 \approx 1.9$, with $A(0) \approx -0.91$. When $\lambda = 1$ the corresponding values given in I were $\Gamma_{\max} = 2.76$, with $A(0) \approx -0.56$ and $X_0 \approx 1.63$. Thus when $\lambda < 1$ neither Γ_+ nor Γ_- achieves such a large maximum as when $\lambda = 1$, though $A(0)$ has a lower minimum, as can be seen from figure 2. The part of the small loop in the curve of $A(0)$ against Γ_- that is drawn here extends from $2.6 < X_0 < 8.5$, i.e. for this range of X_0 there are clearly four values of $A(0)$ for given Γ_-. In these integrations it is felt that graphical accuracy has been achieved especially in that runs were made with 600 points in addition to those with 300 and 150 as in I. In general the range in X was $(-10, 10)$, though this, as in I, was lengthened, scaled and moved to the right as the separation length X_0 became large. However, even with this refinement it was not found possible to increase X_0 beyond about 9.0, at which value the profile for $A(X)$ developed small oscillations near $X = 0$. This did not occur in I for the case of $\lambda = 1$, but it is possible that the added difficulty here is caused by the large value of Γ_+, which by then had reached -100. The profile $A(X)$ was approaching $-X$ for $X < X_0$ as in I, and the variations in this neighbourhood were large. An extension to the right in figure 2 would show that on the lower branch of the curve $\Gamma_+ \to -\infty$ and $A(0) \to 0$ in an oscillatory manner as $X_0 \to \infty$. By the time $\Gamma_+ = -1.0$ on this branch, $X_0 \approx 2.05$, and the asymptotic form for Γ_+ as a function of X_0 is given in §6.

For $\lambda = 1.25$ the plot of $A(0)$ against Γ_- is similar to that for $\lambda = 0.75$, though the small loop is now further from the origin. The maximum value of Γ_- is approximately 3.80, with $A(0) \approx -0.36$ and $X_0 \approx 1.33$. On the small loop $3.1 < X_0 < 8.5$, and again the results become unreliable at $X_0 = 9.0$, with small oscillations developing in $A(X)$ near $X = 0$; by this time the value of Γ_+ was approximately -25. Near the limit of the plot of figure 3 we have $\Gamma_+ \approx 5.73$, with $X_0 \approx 3.2$, and continuation of the graph to the left would show that $\Gamma_+ \to +\infty$ and $A(0) \to 0$ as $X_0 \to \infty$. Again the profiles are approaching $-X$ for $X < X_0$, and the asymptotic limit is also examined below.

6. The limit solutions as $X_0 \to \infty$

For both values of λ under consideration, the numerical solutions indicate that, as X_0, the position of the reattachment point, is tending to infinity, $A(X)$ is approaching a limit solution. This situation appears to be very like that described in I for the case $\lambda = 1$ in that the position of the separation point is tending to $X = 0$ from below and that $A(X)$ is approaching $-X$ for $X < X_0$. Also, in the neighbourhood of $X = X_0$, $A(X)$ seems to jump from $-X_0$ to X_0, though, unlike the case $\lambda = 1$, $A(X)$ does not appear to be linear for $X > X_0$. In addition, it appears that Γ_- is tending to zero from above for both values of λ, but that Γ_+ tends to $-\infty$ for $\lambda = 0.75$ and to $+\infty$ for $\lambda = 1.25$. The analysis below confirms these tendencies and gives formulae for Γ_+ that are in good agreement with the numerical predictions, though we have been unable to obtain formulae for Γ_-. It emerges that in the immediate neighbourhood of X_0 the limit solution is exactly that described in I.

The formulae for Γ_+ are found quite easily for both $\lambda < 1$ and $\lambda > 1$. In each case we assume that, for $X < X_0$, $A(X) \approx -X$, but for $X > X_0$, $A(X) \approx A_0(X)$, where

$$(A_0 + X)(A_0 - \lambda X)^\lambda = \mathscr{G}_1 \quad \text{for } \lambda < 1, \tag{6.1}$$

$$(A_0 + X)(\lambda X - A_0)^\lambda = \mathscr{G}_2 \quad \text{for } \lambda > 1, \tag{6.2}$$

where $\mathscr{G}_1$ and $\mathscr{G}_2$ are constants. The expressions (6.1) and (6.2) satisfy (4.15) with the right-hand sides set equal to zero, and lead to a relative error $O(X_0^{-\frac{1}{2}})$ which is calculated below. If, as is indicated by the numerical work, $A(X)$ increases from $-X_0$ to X_0 in the neighbourhood of X_0, then we have immediately that

$$\left.\begin{aligned} \mathscr{G}_1 &= 2X_0^{1+\lambda}(1-\lambda)^\lambda \quad (\lambda < 1), \\ \mathscr{G}_2 &= 2X_0^{1+\lambda}(\lambda - 1)^\lambda \quad (\lambda > 1). \end{aligned}\right\} \tag{6.3}$$

But (6.1) and (6.2) also yield Γ_+ in terms of $\mathscr{G}_1$ and $\mathscr{G}_2$, with the result

$$\Gamma_+ = (\lambda^2 - 1)\left(\frac{2X_0}{1+\lambda}\right)^{1+1/\lambda}, \tag{6.4}$$

so that $\Gamma_+ \to \infty$ if $\lambda > 1$, but $\Gamma_+ \to -\infty$ if $\lambda < 1$. There is no contradiction with the case $\lambda = 1$ of I, in which $\Gamma_+ \to 0$ as $X_0 \to \infty$, though clearly the double limit requires further investigation if it is thought to be of interest. A comparison between the formula (6.4) and the computed results is given in table 1. The agreement is quite remarkable in view of the expected error in the asymptotic form (6.4), of relative order $O(X_0^{-\frac{1}{2}})$.

In I, $\Gamma_+ = \Gamma_-(= \Gamma)$, and a formula for Γ was obtained on the following lines. Here a similar approach is not so rewarding, and we do not obtain a formula for Γ_-. Essentially it is the extra integral in (4.15) that prevents this, for to evaluate Γ_-, from (4.15*a*) say, we need to know by how much $A(X)$ differs from $-X$ for $X < X_0$ in order to perform the integral over the infinite range. However, the argument below does give an asymptotic formula for $A(0)$ on the lines of that found in I, and also leads to the form of the limit solution in the neighbourhood of $X = X_0$. We note that the assumption $A(X) \approx -X$ for $X < X_0$ implies the assumption that $\Gamma_- \to 0$ as $X_0 \to \infty$. The contribution $O(X_0^{-\frac{1}{2}})$ to the integral on the right-hand side of (4.15) is required, and this is obtained, when $X < X_0$, both from the neighbourhood of $X_1 = X_0$ and for values of $X_1 > X_0$, where $A_0(X_1)$ is given by (6.1) or (6.2). Thus, for $X < X_0$,

$$\int_X^\infty \frac{A''(X_1)\,\mathrm{d}X_1}{(X_1 - X)^{\frac{1}{2}}} \approx \frac{2\lambda}{(X_0 - X)^{\frac{1}{2}}} + \frac{X_0}{(X_0 - X)^{\frac{3}{2}}} + \int_{X_0}^\infty \frac{A_0''(X_1)\,\mathrm{d}X_1}{(X_1 - X)^{\frac{1}{2}}}, \tag{6.5}$$

	$\lambda = 0.75$		$\lambda = 1.25$	
X_0	Γ_{+N}	Γ_{+AS}	Γ_{+N}	Γ_{+AS}
4.0	−15.53	−15.17	7.20	5.52
4.4	−19.00	−18.95	8.24	6.55
4.8	−23.48	−23.22	9.33	7.66
5.2	−28.69	−27.99	10.48	8.85
5.6	−34.22	−33.27	11.70	10.11
6.0	−40.06	−39.08	13.00	11.45
6.5	−48.09	−47.11	14.74	13.22
7.0	−57.02	−56.00	16.60	15.11
7.5	−66.82	−65.78	18.56	17.11
8.0	−77.47	−76.47	20.64	19.21
8.5	−89.01	−88.09	22.83	21.43

TABLE 1. Values of Γ_+ as calculated from the numerical solution of the integral equation (suffix N) and from the asymptotic formula (6.4) (suffix AS) for $\lambda = 0.75, 1.25$

	$\lambda = 0.75$		$\lambda = 1.25$	
X_0	$A_N(0)$	$A_{AS}(0)$	$A_N(0)$	$A_{AS}(0)$
4.0	+0.010	−0.193	−0.035	−0.134
4.4	−0.086	−0.167	−0.086	−0.116
4.8	−0.169	−0.147	−0.114	−0.102
5.2	−0.161	−0.130	−0.103	−0.090
5.6	−0.117	−0.117	−0.079	−0.081
6.0	−0.090	−0.105	−0.066	−0.073
6.5	−0.087	−0.093	−0.062	−0.065
7.0	−0.082	−0.083	−0.058	−0.058
7.5	−0.076	−0.075	−0.053	−0.052
8.0	−0.072	−0.068	−0.050	−0.047
8.5	−0.080	−0.062	−0.054	−0.043

TABLE 2. Values of $A(0)$ as calculated from the numerical solution of the integral equation (suffix N) and from the asymptotic formula (6.7) (suffix AS) for $\lambda = 0.75, 1.25$

where the first two terms are obtained by integrating by parts and noting, from (6.1) and (6.2), that A' jumps from -1 to $2\lambda - 1$ as A jumps from $-X_0$ to X_0. Differentiation of either of (4.15a, b) then leads to a formula for X_2, the separation point where $A(X_2) = 0$, and we have, since $|X_2| \ll 1$,

$$-\lambda X_2 \approx \frac{2\lambda + 3}{4X_0^{\frac{3}{2}}} + \frac{1}{4}\int_{X_0}^{\infty} \frac{A_0''(X_1)\,dX_1}{X_1^{\frac{3}{2}}}. \tag{6.6}$$

Both terms on the right-hand side are $O(X_0^{-\frac{3}{2}})$, and the integral has been evaluated numerically when $\lambda = 0.75$ and $\lambda = 1.25$ by use of (6.1)–(6.3). The results are that

$$X_2 = -1.545X_0^{-\frac{3}{2}} \ (\lambda = 0.75), \quad X_2 = -1.070X_0^{-\frac{3}{2}} \ (\lambda = 1.25); \tag{6.7}$$

when $\lambda = 1.0$ the result in I is that $X_2 = -1.25X_0^{-\frac{3}{2}}$.

In table 2 we present a comparison between X_2 as calculated from (6.7) and $A(0)$ (since $A(X) \approx -X + X_2$ near $X = 0$) as given by the numerical integration of the integral equation. We know from the calculations leading to figures 2 and 3 that $A(0)$ oscillates about its asymptotic form, and this can be seen in table 2. When $\lambda = 0.75$

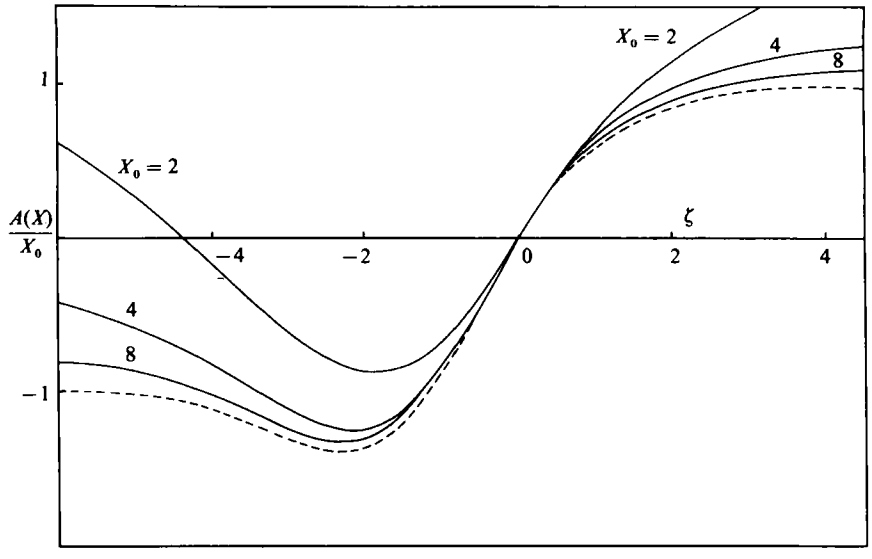

FIGURE 4. The function $A(X)/X_0$ versus ζ for various values of X_0, with $\lambda = 0.75$. The broken line is the limit solution $B(\zeta)$ as calculated in I.

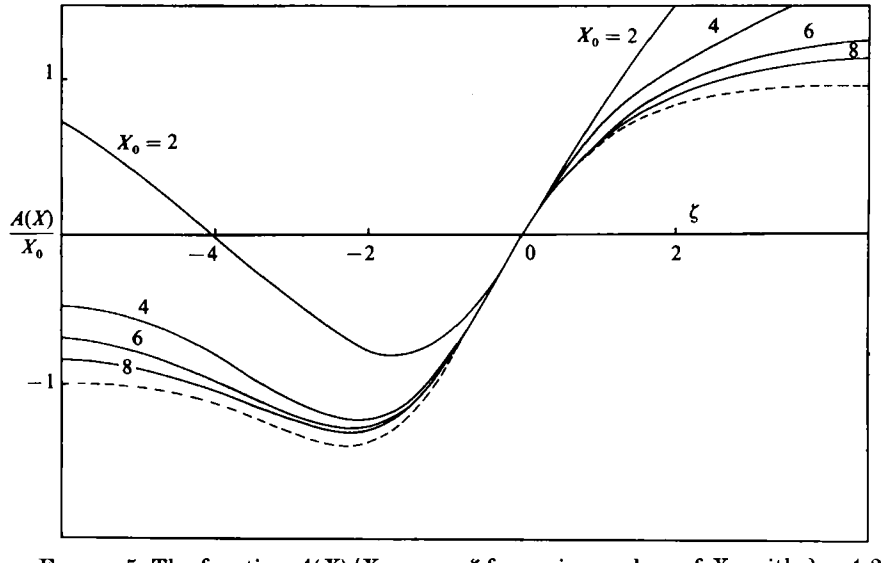

FIGURE 5. The function $A(X)/X_0$ versus ζ for various values of X_0, with $\lambda = 1.25$. The broken line is the limit solution $B(\zeta)$ as calculated in I.

the small loop of figure 2 extends from $2.6 < X_0 < 8.5$ approximately, and when $\lambda = 1.25$ the corresponding range is $3.1 < X_0 < 8.5$. For both values of λ there appears to be another oscillation commencing at $X_0 \approx 8.0$, but it is difficult to be certain about this as the numerical method became inadequate for both values of λ by the time X_0 reached 9, as noted in §5.

To examine the limiting form of A in the neighbourhood of $X = X_0$ we write, in the differentiated form of (4.15), $A(X) = X_0 B(\zeta)$, $\zeta = (X - X_0)X_0^{\frac{1}{2}}$. Retention of the leading terms for $X_0 \gg 1$, and integration with the condition $B(\infty) = 1$, so that $B(\infty) = A(X_0+0)/X_0$, then shows that B satisfies the limiting integral equation of I.

Some properties of this integral equation were given there, and the existence of an eigensolution for large negative ζ that explained the oscillations of $A(0)$ and Γ about their asymptotic forms was demonstrated. This limiting solution, for $A(X)/X_0$ as a function of ζ, is shown in figures 4 and 5 together with the results for $X_0 = 2, 4, 8$ for $\lambda = 0.75, 1.25$ and, in addition, for $X_0 = 6$ when $\lambda = 1.25$, when the approach to the limit is marginally slower.

7. Discussion

The phenomenon of marginal separation occurring on the line of symmetry of a paraboloid at incidence can be clearly seen from figure 4 of Cebeci *et al.* (1980). When the angle of incidence $\alpha_0 = 40°$ the streamwise component of skin friction becomes very small at a point on the leeward line of symmetry before recovering again to positive values (it is the authors' definition of coordinates that makes it convenient for them to plot the wall shear as a negative quantity). Indeed, at $\alpha_0 = 41°$ the separation is no longer marginal and its position terminates the computation. It is evident from their figure 4 that the downstream (increasingly negative p in their notation) gradient of the skin friction is less than the upstream gradient; this corresponds to the situation $\lambda < 1$ of the present study. Confirmation of this is provided by their figure 7, in which the authors plot the crossflow velocity (w being defined in the sense of θ increasing), from which it follows that the configuration is one of outflow from the line of symmetry, i.e. $c_1 > 0$. Since $\tau_2/\tau_1 = 1 - c_1/\tau_1$ ($\equiv \lambda$) the two results are consistent with the theory given here.

In the case $\lambda < 1$ both $\Gamma_\pm$ are bounded above by a positive number. Indeed the non-zero crossflow has limited the parameters Γ_+, as we have seen, even more than in the two-dimensional case; this in a sense is not surprising, as the incipiently separating boundary layer is being emptied of its fluid by the crossflow. In addition, as the separation bubble increases in length ($X_0 \to \infty$), Γ_+ tends to minus infinity, so that the flow downstream of the interaction must be well and truly attached in that the skin friction is above its Goldstein value of λX, though it should be noted that when $\lambda < 1$ the effect of the interaction region is, in terms of Reynolds number, less on the downstream flow than it is on the upstream flow.

The situation $\lambda > 1$ corresponds to inflow on the line of symmetry, and, although Γ_- is bounded above, Γ_+ tends to infinity with the length of the reverse-flow region. Thus the flow downstream of the interaction region can support a skin friction that is below marginal, and the interaction has had a profound effect on the downstream flow. Inflow on the line of symmetry occurs in the collision process on the inner generator of flow in a curved pipe as considered by Stewartson & Simpson (1982) and on the leeside of a cone at incidence (Cebeci *et al.* 1983), and it may be that a solution similar to that given here has some relevance in such situations. However, as the second example is for supersonic flow and in neither case is the singularity of Goldstein form, it is not clear that the comparison is a valid one. Even if it were, probably not too much importance should be attached to the fact that Γ_+ can now tend to plus infinity, because of the possibility of the existence of a singularity at a point just off the line of symmetry. The fact that the interaction considered here is essentially two-dimensional precludes this, and the limitations of such a theory must be borne in mind.

This work was suggested to me some time ago by Keith Stewartson, and I dedicate it to him with my thanks. I am grateful also to Stephen Cowley for his constructive criticism.

REFERENCES

BROWN, S. N. & STEWARTSON, K. 1983 On an integral equation of marginal separation. *SIAM J. Appl. Maths* **43**, 1119–1126.

CEBECI, T., KHATTAB, A. K. & STEWARTSON, K. 1980 On nose separation. *J. Fluid Mech.* **97**, 435–454.

CEBECI, T., STEWARTSON, K. & BROWN, S. N. 1983 Non-similar boundary layers on the leeside of cones at incidence. *Comp. Fluids* **11**, 175–186.

DUCK, P. W. 1984 The effect of a surface discontinuity on an axi-symmetric boundary layer. *Q. J. Mech. Appl. Maths* **37**, 57–74.

GOLDSTEIN, S. 1948 On laminar boundary-layer flow near a point of separation. *Q. J. Mech. Appl. Maths* **1**, 43–69.

KLUWICK, A., GITTLER, P. & BODONYI, R. J. 1984 Viscous–inviscid interactions on axisymmetric bodies of revolution in supersonic flow. *J. Fluid Mech.* **140**, 281–301.

NISHIKAWA, N. & YASUI, Y. 1984 Separation of three-dimensional boundary layers on elliptic paraboloids. *Theoretical & Appl. Mech.* **32**, 79–90.

RHYZHOV, O. & SMITH, F. T. 1985 Short-length instabilities, breakdown and initial value problems in dynamic stall. (To appear in *Mathematika*.)

SMITH, F. T. 1977 The laminar separation of an incompressible fluid streaming past a smooth surface. *Proc. R. Soc. Lond.* A **356**, 433–463.

SMITH, F. T. 1978 Three-dimensional viscous and inviscid separation of a vortex sheet from a smooth non-slender body. *RAE Tech. Rep.* 78095.

SMITH, F. T. 1982 Concerning dynamic stall. *Aero. Q.* 331–352.

SMITH, F. T. & GAJJAR, J. 1984 Flow past wing–body junctions. *J. Fluid Mech.* **144**, 191–215.

SMITH, F. T., SYKES, R. I. & BRIGHTON, P. W. M. 1977 A two-dimensional boundary layer encountering a three-dimensional obstacle. *J. Fluid Mech.* **83**, 163–176.

STEWARTSON, K. 1970 Is the singularity at separation removable? *J. Fluid Mech.* **44**, 347–364.

STEWARTSON, K. & SIMPSON, C. J. 1982 On a singularity initiating a boundary-layer collision. *Q. J. Mech. Appl. Maths* **35**, 1–16.

STEWARTSON, K., SMITH, F. T. & KAUPS, K. 1982 Marginal separation. *Stud. Appl. Maths* **67**, 45–61.

STEWARTSON, K. & WILLIAMS, P. G. 1969 Self-induced separation. *Proc. R. Soc. Lond.* A **312**, 181–206.

SYCHEV, V. V. 1972 On laminar separation. *Izv. Akad. Nauk SSSR, Mekh. Zhid. Gaza* **3**, 47–59.

VATSA, V. N. & WERLE, M. J. 1977 Quasi-three-dimensional boundary-layer separation in supersonic flow. *Trans. ASME* I: *J. Fluids Engng* **99**, 634–000.